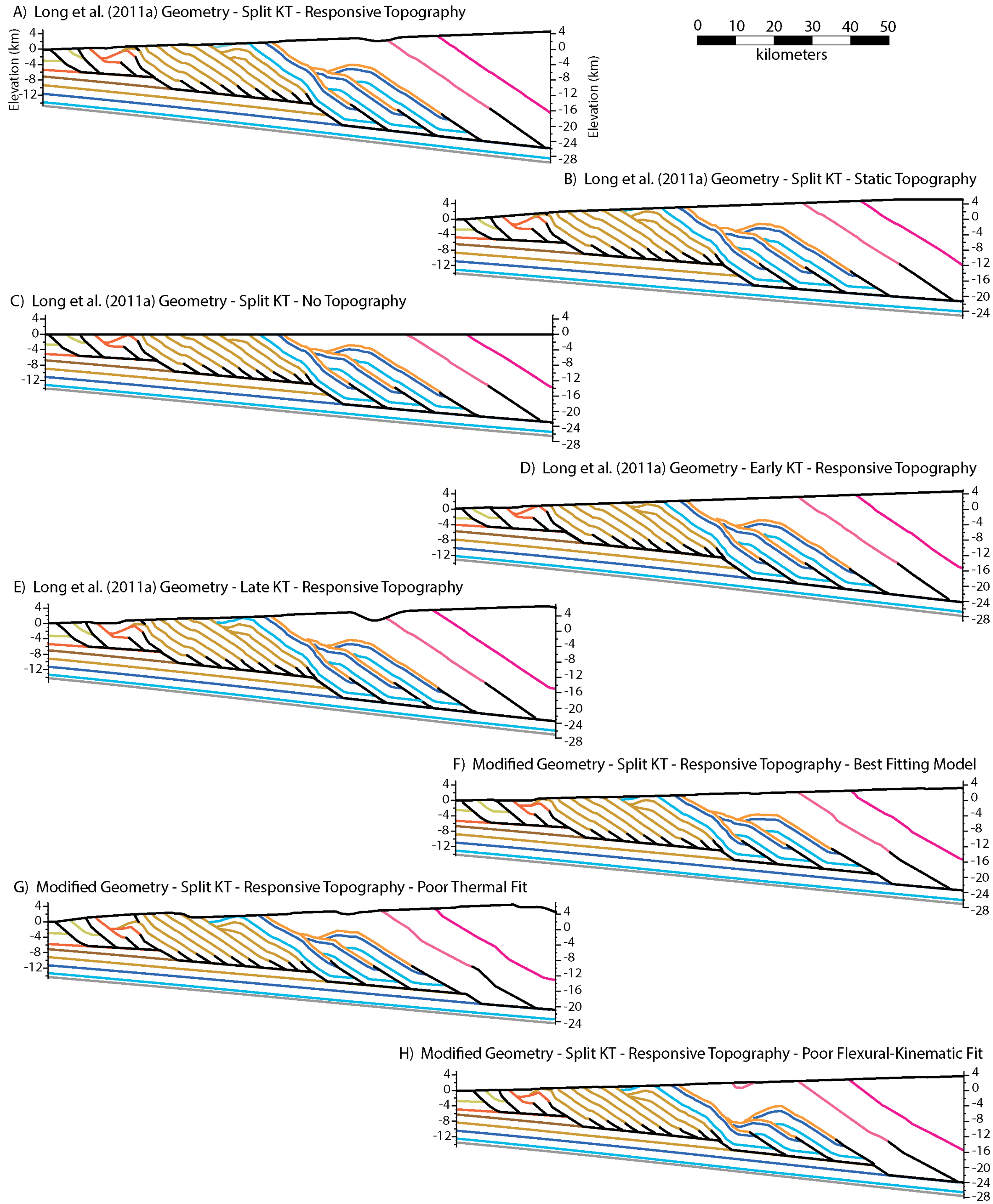

Supplementary Figure 1: Flexural-kinematic modelling output of the present-day Trashigang cross-section for all models presented in sections 4 and 5.

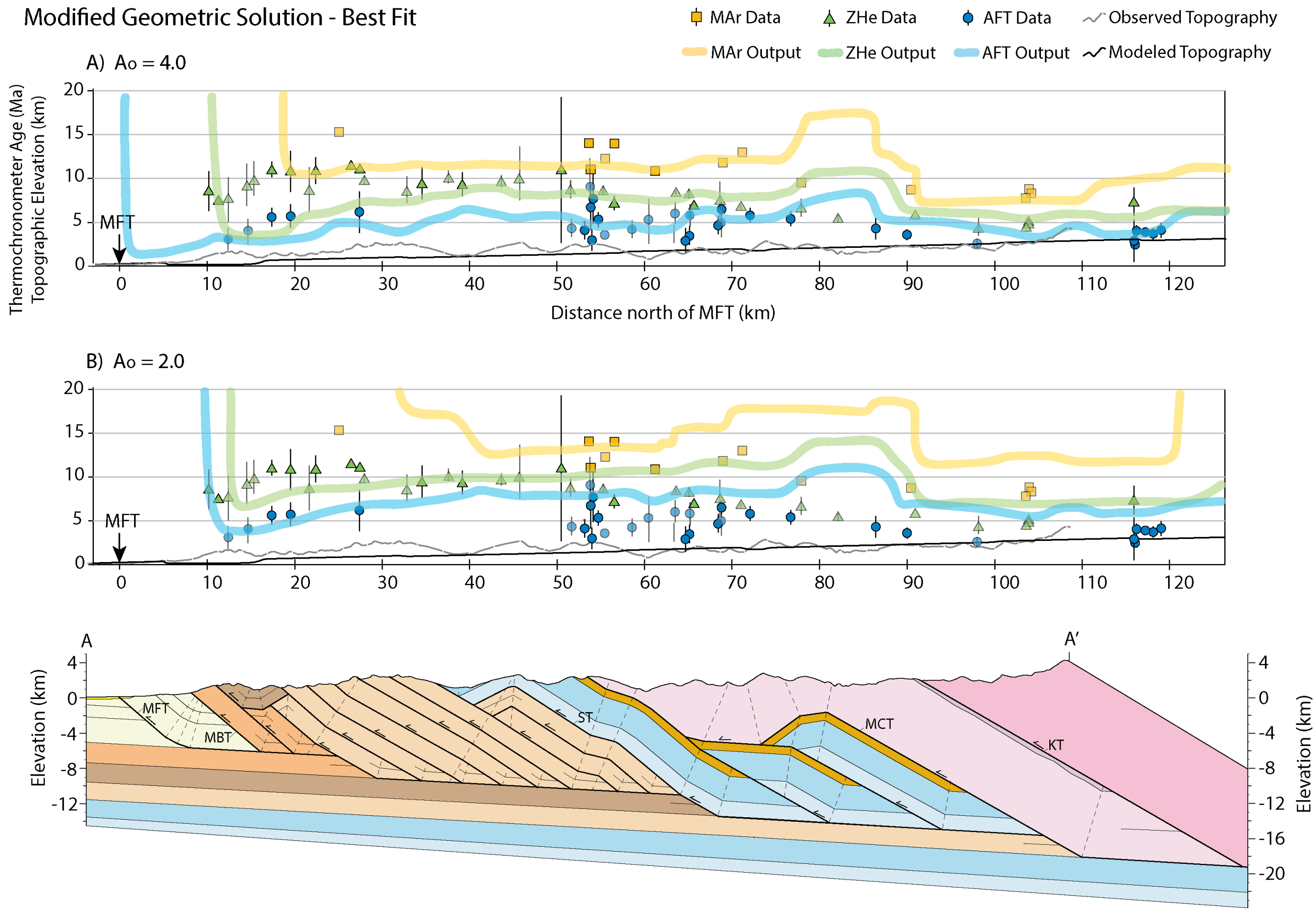

Supplementary Figure 2: Predicted MAr (yellow), ZHe (green), and AFT (blue) cooling ages using a flexural-kinematic model of the modified Trashigang cross-section geometry proposed in this study (Supplementary Figure 1f), preferred shortening rates (Table 3b), and surface radiogenic heat production values of Velocity B, and surface radiogenic heat production values of (A) 4.0 μW/m^3 and (B) 2.0 μW/m^3. The Baxa footwall ramp in the décollement has been shifted 35 km north. Published data include additional ages from the Kuru Chu line of section west of the Trashigang section (Long et al., 2012), shown in the graphs with lighter-colored symbols. The flexural-kinematic model used a Split KT kinematic scenario and Responsive topography.

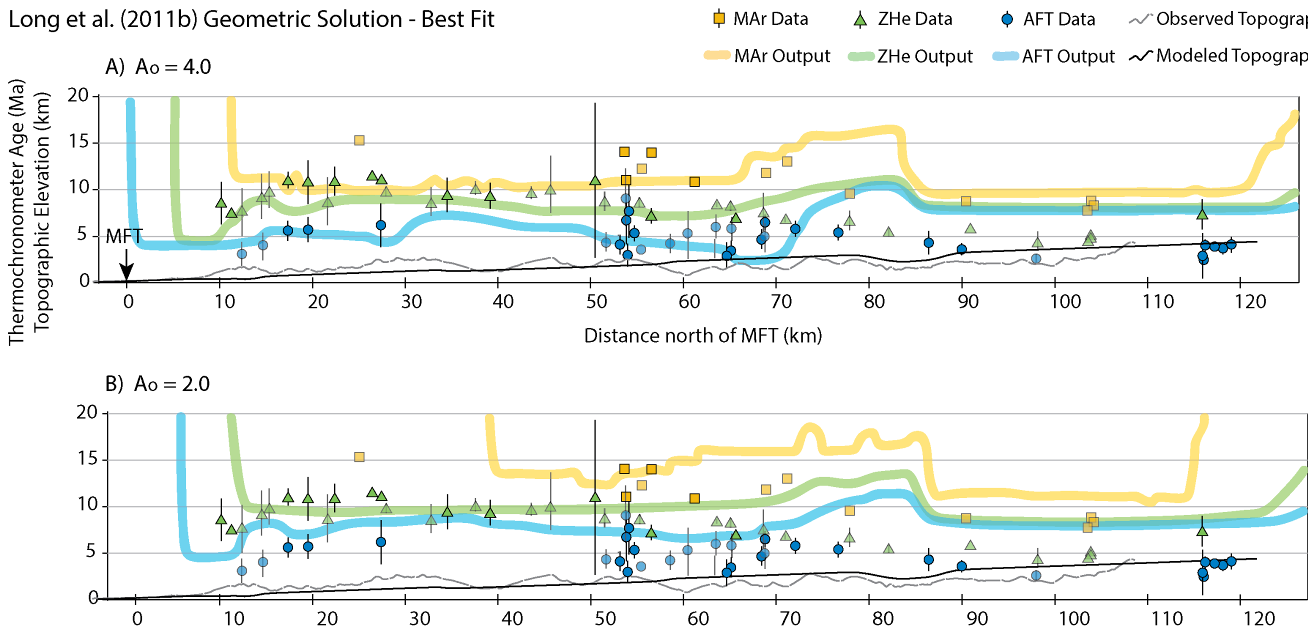

Supplementary Figure 3: Predicted MAr (yellow), ZHe (green), and AFT (blue) cooling ages using the Trashigang cross-section geometry originally proposed by Long et al. (2011a), Velocity B, and surface radiogenic heat production values of (A) 4.0 µW/m^3 and (B) 2.0 µW/m^3 . Published data include additional ages from the Kuru Chu line of section west of the Trashigang section (Long et al., 2012), shown in the graphs with lighter-colored symbols. The flexural-kinematic model used a Split KT kinematic scenario and Responsive topography (Supplementary Figure 1a).

Study	Sample	Unit	Elevation (m)	Longitude (°E)	Latitude (°N)	Central AFT Age (Ma)	2σ Analytical Error (Ma)	Mean ZHe Age (Ma)	2σ Variability Range (Ma)	Reported MAr Age (Ma)	2σ Analytical Error (Ma)
Stuwe & Foster (2001)*	8	GHlo	2540	91.53157	27.24116	-	-	-	-	14.1	0.2
Stuwe & Foster (2001)*	9	GHlo	2480	91.52660	27.24549	3.1	1.2	-	-	11.1	0.4
Stuwe & Foster (2001)*	11	GHlo	1750	91.54075	27.27539	-	-	-	-	14.1	0. 4
Stuwe & Foster (2001)*	12	GHlo	1060	91.54378	27.32288	-	-	-	-	11.0	0.4
Grujic et al. (2006)	BH53	GHlo	2405	91.548083	27.237361	6.9	2.6	-	-	-	-
Grujic et al. (2006)	BH52	GHlo	2350	91.554667	27.236056	7.8	2.8	-	-	-	-
Grujic et al. (2006)	BH60	Pzj	795	91.480667	27.282361	4.2	1.0	-	-	-	-
Grujic et al. (2006)	BH61	GHlo	780	91.491000	27.303417	5.4	0.8	-	-	-	-
Grujic et al. (2006)	BH90	GHlo	910	91.574528	27.344972	3.6	1.0	-	-	-	-
Grujic et al. (2006)	BH64	GHlo	825	91.554472	27.350056	3.0	1.4	-	-	-	-
Grujic et al. (2006)	BH324	GHlo	1995	91.59683	27.374361	4.8	1.0	-	-	-	-
Grujic et al. (2006)	BH94	Pzc	2050	91.599833	27.375333	6.6	0.8	-	-	-	-
Grujic et al. (2006)	BH100	GHlo	905	91.563722	27.411389	5.9	0.8	-	-	-	-
Grujic et al. (2006)	BH72	GHlo	1420	91.554722	27.465000	5.5	0.8	-	-	-	-
Grujic et al. (2006)	BH66	GHlo	930	91.561139	27.551361	4.4	1.2	-	-	-	-
Grujic et al. (2006)	BH70	GHlo	1760	91.499528	27.584167	3.7	0.6	-	-	-	-
Long et al. (2012)	BU07-53	Pzg	655	91.48011	26.86572	-	-	8.65	2.22	-	-
Long et al. (2012)	BU07-54	Pzd	700	91.48028	26.87497	-	-	7.61	0.28	-	-
Long et al. (2012)	BU07-33	Pzd	1710	91.54794	26.93311	5.69	1.04	11.12	0.85	-	-
Long et al. (2012)	BU07-35	Pzb	1580	91.54761	26.95992	5.82	1.28	10.91	2.29	-	-
Long et al. (2012)	BU07-36	Pzb	1785	91.53083	26.97442	-	-	11.00	1.47	-	-
Long et al. (2012)	NBH-18	Pzb	1815	91.52072	27.01200	-	-	11.60	0.03	-	-
Long et al. (2012)	BU07-37	Pzb	2385	91.50142	27.02675	6.27	2.34	11.25	0.50	-	-
Long et al. (2012)	BU07-42	Pzb	2165	91.52089	27.08486	-	-	9.54	1.82	-	-
Long et al. (2012)	BU07-43B	Pcd	2315	91.56708	27.13450	-	-	9.43	1.33	-	-
Long et al. (2012)	BU07-55	Pzj	2350	91.52122	27.24222	-	-	11.07	8.27	-	-
Long et al. (2012)	BH-57	Pcd	605	91.44656	27.27869	-	-	7.30	0.77	-	-
Long et al. (2012)	BH-78	Pzc	1000	91.63897	27.35144	-	-	7.09	0.28	-	-
Coutand et al. (2014)	BH-363	GHh	3610	91.37263	27.96956	2.5	0.4	-	-	-	-
Coutand et al. (2014)	BH-351	GHh	3870	91.30357	27.97318	3.0	2.4	-	-	-	-
Coutand et al. (2014)	BH-352	GHh	3880	91.29016	27.97416	4.1	0.6	-	-	-	-
Coutand et al. (2014)	BH-357	GHh	4085	91.29827	27.98563	4.0	0.4	7.42	1.56	-	-
Coutand et al. (2014)	BH-355	GHh	4275	91.2987	27.99005	3.8	0.6	-	-	-	-
Coutand et al. (2014)	BH-362	GHh	4300	91.29901	27.99750	4.2	0.8	-	-	-	-

Supplementary Table 1: Thermochronometer sample locations and reported cooling ages used in this study. Reported AFT and MAr data include 2σ analytical error. ZHe ages are based on the mean reported age among all aliquots for each sample; 2σ range shown for ZHe includes variability among aliquots. *Latitude and longitude of samples from Stüwe and Foster (2001) were estimated using ESRI ArcMap WGS84 datum.